Feature Article

Monte Carlo simulation studies of the interfaces between polymeric and other solids as models for fiber-matrix interactions in advanced composite materials

Jörg Baschnagel[a], *Kurt Binder**

Institut für Physik, Johannes Gutenberg Universität Mainz,
Staudinger Weg 7, D-55099 Mainz, Germany

(Received: November 21, 1995)

SUMMARY:

As a coarse-grained model for dense amorphous polymer systems interacting with solid walls (i. e., the fiber surface in a composite), the bond fluctuation model of flexible polymer chains confined between two repulsive surfaces is studied by extensive Monte Carlo simulations. Choosing a potential for the length of an effective bond that favors rather long bonds, the full temperature region from ordinary polymer melts down to the glass transition is accessible. It is shown that in the supercooled state near the glass transition an "interphase" forms near the walls, where the structure of the melt is influenced by the surface. This "interphase" already shows up in static properties, but also has an effect on monomer mobilities and the corresponding relaxation behavior of the polymer matrix. The thickness of the interphase is extracted from monomer density oscillations near the walls and is found to be strongly temperature dependent. It is ultimately larger than the gyration radius of the polymer chains. Effects of shear deformation on this model are simulated by choosing asymmetric jump rates near the moving wall (large jump rate in the direction of motion, and a small rate against it). It is studied how this dynamic perturbation propagates into the bulk of the polymer matrix.

1. Introduction

When one considers composite materials where fibers (such as quartz, carbon, metal, etc.) are embedded in amorphous polymer matrices[1–7], the interfacial region controls many of the properties of the material, such as formation of cracks and crazes, and other mechanical and thermal properties. There is various indirect evidence that this interfacial region can be considered as a kind of mixed phase — it is called[7] the "interphase". Thus it is potentially important for applications to improve the understanding of structure-property relationships particularly of this region (see Fig. 1)[8].

Other situations which are potentially very interesting for many applications are thin polymeric films on various solid substrates. There is a huge experimental and theoretical activity on this subject, see, e. g., refs.[9–15] This problem presents also a

[a] Present address: Institut Charles Sadron, 6 rue Boussingault, F-67083 Strasbourg Cedex, France.

 CCC 1022-1344/96/$05.00

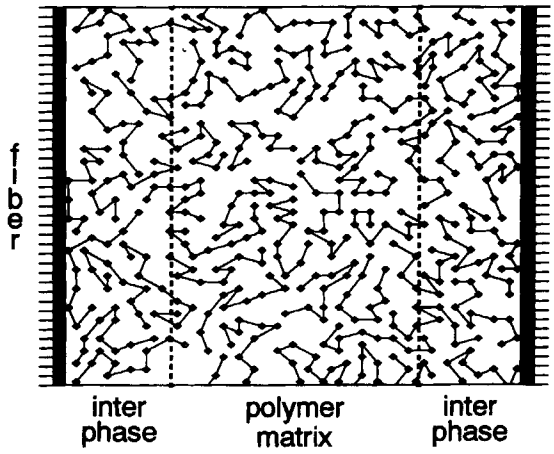

Fig. 1. Schematic illustration of the interphase between a fiber component and an amorphous polymer matrix (following Drzal[7], in changed form). The interaction between the fiber and the polymer (modelled by a pure hard-core repulsion in the present simulations) influences strongly the structure and the mobility of the polymer melt within the "interphase", whereas the macromolecules sufficiently away from the fiber surfaces behave like chains in the unconstrained bulk material. (From Baschnagel and Binder[8])

basic challenge to fundamental science, and our model study may give additional insight into this problem, too.

In the present paper, we are not attempting a "molecular modeling" approach of the solid-polymer interface on an atomistic scale. Since the thickness of the "interphase" in Fig. 1 is estimated to be of the order of[7] 10 nm, the linear dimensions that must be treated are relatively large-scale, which allows to work with simplified, coarse-grained (lattice) models to study the general features of a confined polymer melt. Although these coarse-grained models mimic the specific interactions between the polymer and the fiber component of real materials only in a fairly crude fashion, they exhibit the great advantage that they can be simulated very efficiently. Thus it becomes possible to investigate equilibrium properties and to monitor relaxation processes at low temperatures, which are difficult to access in chemically realistic simulations[11]. Already on a very crude level of modeling, where the surfaces of the fibers are simply described by parallel flat hard walls[8,16,17], a pronounced effect on the structure[8] and dynamics[16,17] of the polymers in this "interphase" region occurs. We attempt to interpret this wall effect, that ultimately is responsible for the existence of this special "interphase", qualitatively in terms of simple entropic effects: the fiber influences the neighboring polymeric material via the interplay of "packing effects" of the monomers near the wall[11,18–25] and the decrease of configurational entropy of the polymers when one cools the matrix towards its glass transition. Such an entropy decrease is known from experiment to occur in the bulk[26–28] and is reproduced by the simple model used here[29].

The outline of this paper is now as follows. In section 2 we describe the model and the simulation method. The properties of the polymer melt in the bulk are summarized in section 3, since the key point of the present work is to contrast the behavior near the hard walls to the behavior in the bulk. Section 4 then describes the static structure of the interphase region in detail, while section 5 analyzes the dynamical properties in this region, focusing in the constraints due to the fiber surface on both parallel and perpendicular motions, which are characterized by monomer mean square displacements and relaxation times. Section 6 is concerned with the modeling of shear effects, assuming that one wall moves at constant velocity while the opposite wall is at rest. Since our Monte Carlo model lacks any direct account of hydrodynamic interactions, we model the shear forces on the monomers near the moving wall simply via an asymmetry of jump rates (jump rates against the flow are distinctly smaller than in the direction of the velocity field). Section 7 finally presents a summary and outlook on future work.

2. The bond fluctuation model and some comments on the Monte Carlo simulation technique

The bond fluctuation model[30-34] is one of the most popular lattice models for the dynamic Monte Carlo simulation[35] of dense macromolecular systems: it has been used to model polymer blend thermodynamics[32,36-40], polymer brushes[41-46], and the glass transition[47-53], etc. Thus we only summarize the most salient features here.

Image a "coarse-graining" where we combine n chemical monomers (monomer units) along the backbone of a chain into an "effective bond" connecting "effective monomers"[40,54-57], see Fig. 2. Thus, in this schematic example for a polyethylene chain the covalent C—C bonds 1, 2, 3 are forming the effective bond I, covalent bonds 4, 5, 6 are forming the effective bond II, etc. A similar "mapping" may be carried out for other polymers as well, and in fact has been carried out for polycarbonate[58-60], but this is outside of consideration here. In every case, the end-to-end distance of a group of successive chemical bonds of a flexible polymer chain may fluctuate, depending on the conformation state of these bonds (assuming temperatures high enough that also relative minima of the torsional potential are populated). This fluctuation of the end-to-end distance of such a group of bonds is translated into a fluctuation of the length of the effective bond, b. In practice we use[36] $2 \leq b \leq \sqrt{10}$ with the exclusion of the bond length $b = \sqrt{8}$ (all lengths being measured in units of the lattice spacing), because then the excluded volume constraint suffices to guarantee that bonds can never cross in the course of the random motion of the polymers. The dynamics of the chains is not modelled fully, of course: we completely disregard vibrations of bond lengths, bond angles, etc., and focus only on random hopping events over the barriers of the torsional potential. E.g., in the case of polyethylene, these motions are random jumps from the *trans* (t) minimum to one of the *gauche* states (g_+, g_-) or vice versa. These conformational transitions are "translated" into the coarse-grained lattice model by carrying out a random hopping of the effective monomers by one lattice constant in the $\pm x$, $\pm y$, or $\pm z$ direction. I.e., one effective monomer and as well one of the six directions is randomly chosen, and a corresponding

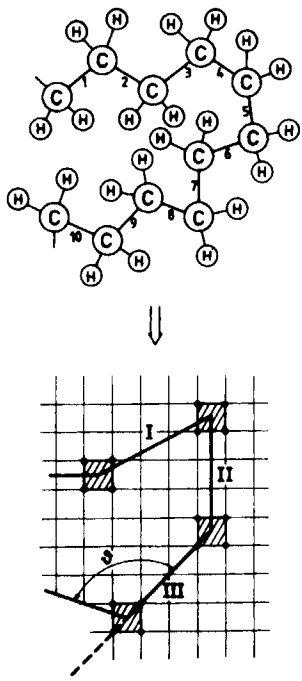

Fig. 2. Approximate mapping of a chemically realistic polymer (e.g. polyethylene) to the bond fluctuation model. We combine n successive chemical bonds along the backbone of the chain (e.g., $n = 3$ here) into one "effective bond" between "effective monomers". To simulate excluded volume interactions, each effective monomer blocks eight sites at the corner of an elementary cube on the simple cubic lattice from further occupation (only for simplicity, rather a square lattice is shown here). Potentials $U_{\text{eff}}(b)$ for the length of an effective bond, or $V_{\text{eff}}(\vartheta)$ for the angle ϑ between two subsequent effective bonds, may be constructed such that the geometrical characteristics of the chemically realistic chain (e.g., gyration radius, persistence length, etc.) are correctly reproduced. (From Baschnagel et al.[54])

displacement of the effective monomer is attempted. Of course, the move is acceptable only, if it does not violate the excluded volume constraint, and if the neighboring bond vectors connecting to that monomer still belong to the allowed set of bond vectors. In the presence of potentials (for lengths of effective bonds, the angles between them, and/or intermolecular potentials, respectively) one has to compute the transition probability $W = \exp(-\delta\mathcal{H}/(k_B T)$ where $\delta\mathcal{H}$ is the energy change associated with this move. Only if W exceeds a random number, uniformly distributed between zero and unity, the move is carried out (standard Metropolis-type Monte Carlo sampling[35]). As is well-known, this algorithm ensures thermal equilibrium at the chosen absolute temperature T, but the time unit (1 attempted Monte Carlo step per monomer = 1 MCS) is related to physical time with an unknown conversion factor only (in general, this conversion factor is temperature dependent, but typically 1 MCS may correspond to 10^{-11} s). Although this dynamic Monte Carlo algorithm is only a crude simplification of all the rich variety of motion that occurs in actual polymer melts and polymer glasses, it nevertheless represents the large scale motions of polymer chains rather faithfully[35,57], and reproduces either the Rouse model[61,62] (for short enough chains) or the reptation model[62] (for long chains), respectively.

Although the algorithm described above performs very fast (several millions of attempted moves are carried out on CRAY-YMP processors[31], and the speed on RISC workstations is only about one order of magnitude less), typical runs (choosing lattices of size 40^3, for instance, noting[58] that one lattice spacing roughly corresponds to a physical distance of 2 Å) can cover 7 orders of magnitude of Monte Carlo time, and

thus span a range that is much shorter (e. g., from 10^{-11} to 10^{-4} s) than the time range accessible to real experiment. If the above algorithm is used for cooling the system near and through the glass transition, pronounced effects due to the large cooling rate do occur[48]: compared to real experiments, the simulation quenches the melt down extremely rapidly. The computer-generated model polymer melts near the glass transition thus are clearly less well equilibrated than their experimental counterparts[48]. To some extent, however, this problem can be circumvented by equilibrating the melt with a physically artificial algorithm, such as so-called "slithering snake" moves where a bond is removed from one chain end and attached to the other end in a randomly chosen direction. This method of equilibration indeed is advantageous in a variety of situations[39,51] and has been used in the present study for the equilibration and the analysis of static properties throughout. In practice one even uses a "hybrid" algorithm, where the "random hopping" moves and the "slithering snake" moves are randomly mixed[51]. When one feels that the system is well enough equilibrated, a clock is turned to zero and "time averaging" begins, forbidding any further "slithering snake" motions; thus the study of dynamic properties can be separated from the study of static ones[35].

In the present work, only the simplest possible choice for the potentials is used: intermolecular potentials are all put equal to zero except for excluded volume, and also the effective bond angle potential $V_{\text{eff}}(\vartheta)$ is put equal to zero (while both $U_{\text{eff}}(b) \neq 0$ and $V_{\text{eff}}(\vartheta) \neq 0$ must be used if a modeling of real specific polymers is attempted[58,59]). Here we are only concerned with the most general features of the problem, and use a two-state effective bond-Hamiltonian $\mathscr{H}(\boldsymbol{b})$ (Fig. 3): $\mathscr{H}(\boldsymbol{b}) = 0$ for bond vectors belonging to the set of groundstate bonds $\{\boldsymbol{b} = (\pm 3, 0, 0), (0, \pm 3, 0), (0, 0, \pm 3)\}$, while $\mathscr{H}(\boldsymbol{b}) = \varepsilon$ in all other cases. We choose units such that $k_B = 1$, $\varepsilon = 1$, and hence $k_B T/\varepsilon$ is in the following written as a dimensionless normalized temperature T to abbreviate the notation.

The choice shown in Fig. 3 is physically motivated, since on cooling for most polymers the persistence length increases (e. g., short pieces of a polyethylene chain go into the all-*trans* state), and thus it is natural to create an enthalpic preference for rather long effective bonds. But this choice automatically has the effect that a "conflict" is created between the "desire" of bonds to reach their ground state and the necessity to pack monomers locally as densely as possible in a dense polymeric melt. Any bond that takes its groundstate length "wastes" four lattice sites (Fig. 3), which are blocked for the occupation by any other monomers. They do not fit in because of the excluded volume interaction that allows each lattice site to belong to a single monomer only. In a dense system, not all monomers will find space such that all bonds reach their groundstate: this effect is called "geometric frustration"[48-53] and is responsible for the glass transition of the model.

3. Properties of the polymer melt near the glass transition in the bulk

In the polymer melt, the chains are random-walk-like coils and since the density of monomers of one coil inside the gyration radius is much smaller than the melt density itself, the coils must strongly penetrate into each other. A direct look on snapshot

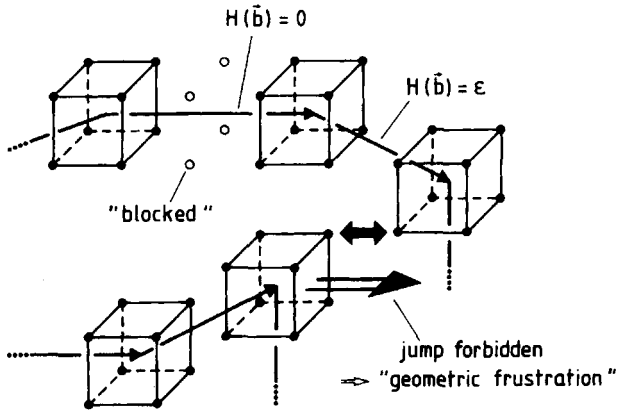

Fig. 3. Sketch of a possible configuration of effective monomers belonging to different chains in the melt in order to illustrate the effect of the "Hamiltonian" $\mathscr{H}(\tilde{b})$ that favors bonds of length $b = 3$ in lattice axis directions. All bond vectors shown in this figure have the energy $\varepsilon = 1$ except the vector (3, 0, 0), which belongs to the groundstate. This vector blocks four lattice sites (marked by ○) which are no longer available to other monomers, since two monomers may not overlap. Due to this excluded volume interaction the jump in the direction of the large arrow is also forbidden. (From Baschnagel et al.[48])

pictures of configurations of our model (Fig. 4) supports this picture. As long as these chains are flexible enough, they still can move and the dynamic properties are in reasonable accord[33,34] with the theoretical description[62]. But when more and more bonds go into their groundstate, the chains locally stiffen and block some motions also in their environment. When this blocking of motions extends over the whole system the melt freezes in its glassy amorphous state. Although this picture of the glass transition of polymer melts resulting from our simulation is clearly oversimplified, our model captures the essential physics!

We first summarize the static properties. Fig. 5 shows the collective structure factor. These data have been generated using a "slow cooling" procedure, increasing the inverse temperature linearly with time according to

$$1/T(t) = \Gamma_Q \, t/T_f \qquad T_f = 0.05 \tag{1}$$

where the quench rate Γ_Q was varied from $\Gamma_Q = 4 \cdot 10^{-5}$ (fast cooling) to $\Gamma_Q = 4 \cdot 10^{-7}$ (slow cooling); T_f is the final temperature. It is seen that the static structure factor has very little temperature dependence, apart from large scattering vectors q which are not of physical interest (remember that $q = 2\pi$ corresponds to distances of one lattice spacing, and on such small scales lattice artefacts are inevitable for our lattice model). Note that the structure factor is defined as

$$S(q) = \frac{1}{NP} \sum_{n,m=1}^{NP} [\langle \exp[i\boldsymbol{q} \cdot (\boldsymbol{r}_{nc} - \boldsymbol{r}_{mc})] \rangle_c]_q \tag{2}$$

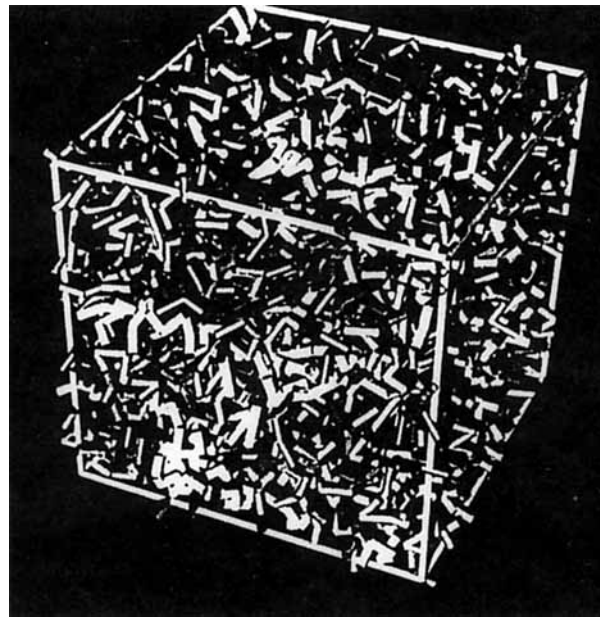

Fig. 4. Snapshot picture of the polymer configuration in a dense melt according to the bond fluctuation model. Each effective bond is shown as a small cylinder, while the effective monomers are not shown in order to simplify the picture. The simulation box shown here is of size 40 × 40 × 40 lattice spacings, and periodic boundary conditions are applied. At the chosen volume fraction $\phi = 0.5$ of occupied lattice sites shown here one has already a dense filling of space by random-walk-like chains

where r_{nc} is the vector to the center of gravity of the n-th monomer in configuration c, $\langle \ldots \rangle_c$ represents the average over all independent configurations (160 of them were used), and the symbol $[\ldots]_q$ stands for the lattice analog of a spherical average in the continuous reciprocal space. In Fig. 5, we have used a chain length $N = 10$ (this is just enough that the single chain structure factor is well approximated[49] by the Debye function[63], Fig. 6) and the number of polymers P then is $P = 180$ in a 30 × 30 × 30 lattice. One sees that $S(q)$ is very small and flat for small q, indicating that polymer melts are nearly incompressible, in agreement with experiment. Near $q \approx 3$ (i.e., about 1.5 Å^{-1}, if a lattice spacing corresponds to 2 Å in real space[58, 59]) a diffuse peak in the scattering intensity appears, the so-called "amorphous halo", and indeed this behavior is in striking agreement with experiment.

While the global structure of the polymer melt is nearly independent of temperature in the bulk, there is some effect on a local scale due to the tendency of the bonds to reach their groundstate, and the resulting local stiffening of the chains. This behavior is seen very clearly in the mean-square bond length[48] $\langle b^2 \rangle$, see Fig. 7. Here also the dependence on the cooling rate is analyzed. In the high temperature region ($T \in [0.6, 2.0]$) the curves for the different cooling rates nicely collapse, indicating that the melt is in a thermally equilibrated liquid state. In this state the chains are mobile enough to respond easily to the speed by which the temperature is reduced. The effect of the finite cooling rate starts to be felt below $T \approx 0.5$ and is accompanied by a strong

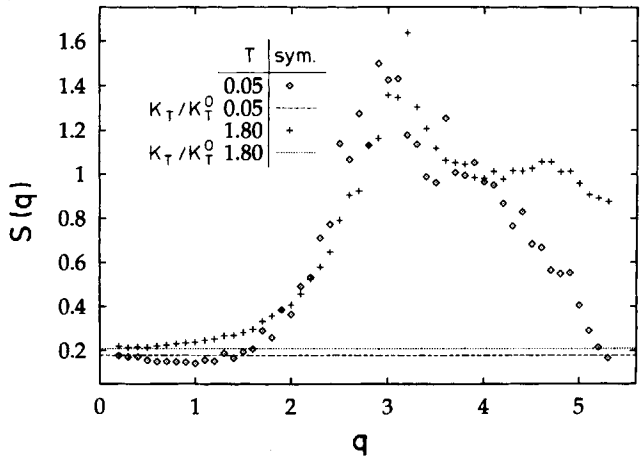

Fig. 5. Plot of the collective static structure factor $S(q)$ vs. wavenumber q for the temperatures $T = 0.05$ (diamonds) and $T = 1.8$ (crosses), applying an intermediate cooling rate $\Gamma_Q = 4 \cdot 10^{-6}$. Additionally, a dashed and a dotted horizontal line are shown which correspond to the normalized static compressibility κ_T/κ_T^0 calculated by a block analysis method (sampling density fluctuations in subblocks of the total system). Here κ_T^0 is the isothermal compressibility of an ideal gas, $\kappa_T^0 = (T\rho)^{-1}$, ρ being the average density of monomers (i.e., $\rho = \phi/8$ because each monomer takes 8 lattices sites), and $\phi = 0.533$ was used. (From Baschnagel and Binder[49])

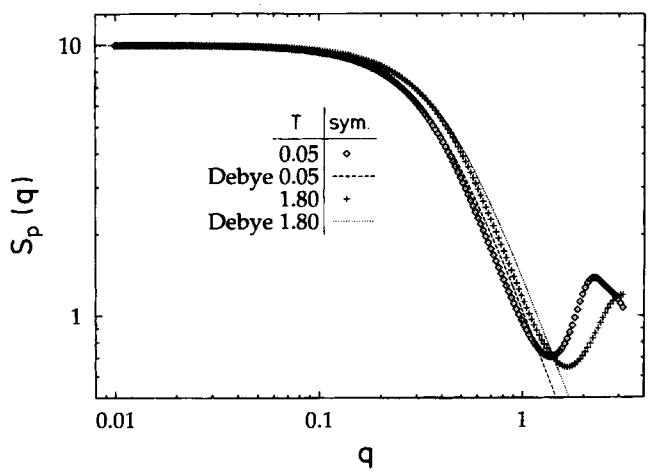

Fig. 6. Temperature dependence of the static structure factor of a polymer $S_p(q)$ and comparison of $S_p(q)$ with the Debye formula[63], $S_p^{DE}(q) = 2N[\exp[-q^2\langle R_g^2\rangle] - 1 + q^2\langle R_g^2\rangle]/[q^2\langle R_g^2\rangle]^2$, $\langle R_g^2\rangle$ being the mean-square gyration radius of the chains. $S_p(q)$ is defined by analogy with Eq. (2), except that the sum runs over monomers of a single chain only, and the result is averaged over all chains. As in Fig. 5, the diamonds and crosses correspond to simulation results at $T = 0.05$ and $T = 1.8$. For computing the Debye formula the values of $\langle R_g^2\rangle$ observed in the simulation at the respective temperatures were used. (From Baschnagel and Binder[49])

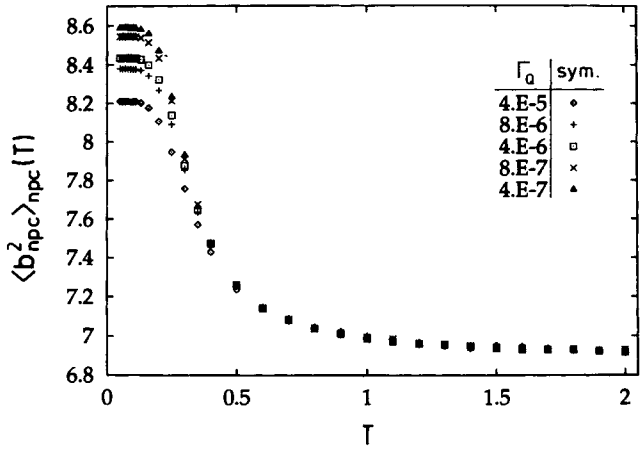

Fig. 7. Plot of the mean-square bond length vs. temperature for five different cooling rates. Data are averaged over 160 statistically independent configurations c, all $N = 10$ monomers of each chain and all $P = 180$ polymers in each simulation box, as symbolically indicated by the indices *npc*. (From Baschnagel et al.[48])

expansion of the mean bond length. The increase of $\langle b^2 \rangle$ continues until the temperature reaches $T \approx 0.2$, where the curves level off. In this temperature range the intrinsic relaxation times of the melt become comparable to the observation time which is determined by the cooling rate. Then the system falls out of equilibrium and $\langle b^2 \rangle$ in the low temperature region ($T \leq 0.2$) increases with decreasing cooling rate, but stays smaller than $\langle b^2 \rangle = 9$, the value reached if all bonds were in their ground state.

The fact that our model really reproduces the glassy freezing in of polymer melts in excellent qualitative agreement with experiment is seen when one examines the incoherent intermediate scattering function[64,65] $\phi_q^s(t)$ (this quantity can be directly compared to inelastic neutron scattering data[66]). Fig. 8 shows corresponding simulation data[64]. One sees that a two step relaxation process develops — the first step and the crossover to the final decay ("β-relaxation") correspond to the "rattling motion" of the effective monomers in the "cages" formed by their environment, the final decay ("α-relaxation"[67]) to the structural relaxation of the polymer melt. This behavior can be accounted for in detail[64,65] by the mode-coupling theory[67] of the glass transition, just as the corresponding experiments[66].

Since in the Monte Carlo simulation a rather short time window is available only, as pointed out above, estimation of the glass transition temperature T_g is fairly difficult, since the system starts to fall out of equilibrium at temperatures far above T_g already (Fig. 7). Using the diffusion constant of the chains in the region of intermediate temperature, $T \geq 0.25$, a fit to a Vogel-Fulcher law[68]

$$D_N(T) = D_N(\infty) \exp[-A/(T - T_0)] \tag{3}$$

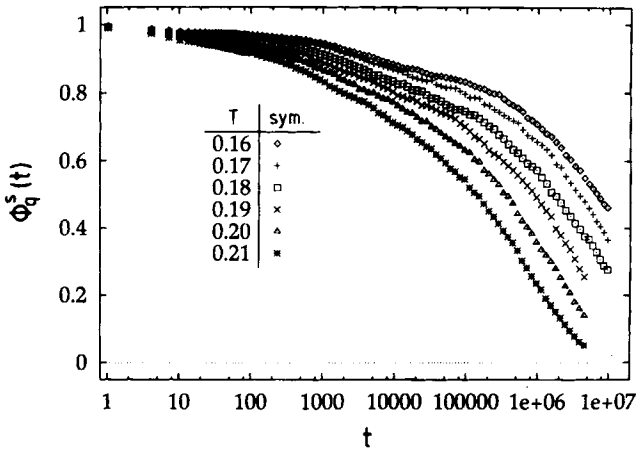

Fig. 8. Simulation data of the intermediate incoherent scattering function $\phi_q^s(t)$, averaged over 16 statistically independent configurations of 180 chains of length $N = 10$, calculated at the maximum of the static structure factor $q = 2.92$, for six different temperatures using the slowest cooling rate and equilibrating the data further to eliminate most of the cooling rate effects. (From Baschnagel[64])

gave a Vogel-Fulcher temperature of $T_0 \approx 0.17$[48]. However, analysis of the dynamic structure factor (Fig. 8) yielded[64,65] a critical temperature of the mode-coupling theory[67] as $T_c \approx 0.15$. However it is clear that T_c is above the glass transition temperature T_g and not below it[66,67], while T_0 always should be a lower bound[26-28] for T_g. Thus estimate for T_0 quoted above[48] should not be taken seriously, since it clearly was obtained from a fit in a rather inappropriate temperature regime, and should rather be interpreted in a sense as a crossover temperature, below which the slowing down associated with the glass transition sets in. A recent re-analysis of the viscosity and dielectric relaxation of many polymer melts[69] also has shown that sometimes the high temperature regime can indeed be fitted to Eq. (3) as well, but the T_0 resulting from such a fit would overestimate T_g distinctly, and can be taken as a kind of crossover temperature only.

However, noting that all evidence shows that for sufficiently short chains in supercooled melts the Rouse model[61,62] is valid[53], i.e. selfdiffusion constant $D_N(T)$ and relaxation time τ_N scale as

$$D_N(T) \sim \langle b^2 \rangle W(T)/N \qquad \tau(T) \sim [W(T)]^{-1} N^2 \tag{4}$$

it is permissible to estimate the glassy relaxation from the Rouse rate W directly, which also should then follow a Vogel-Fulcher law,

$$W(T) = W(\infty) \exp[-A/(T - T_0)] \qquad A = \text{const.} \tag{5}$$

Note that $D_N(T)$ can only be used if one is able to follow the mean-square displacement $g_3(t)$ of the center of gravity of the chains for time $t \gg \tau_N$, i.e. one uses the Einstein relation[40, 53, 62]

$$D_N(T) = g_3(t)/(6t) \qquad t \gg \tau_N \qquad g_3(t) \equiv \langle [r_{CM}(t) - r_{CM}(0)]^2 \rangle \tag{6}$$

where $r_{CM}(t)$ is the center of mass position of a chain at time t. Times $t < \tau_N$ cannot be used, since $g_3(t)$ in dense polymer systems exhibits some anomalous diffusion[34], $g_3(t) \sim t^{x_3}$ with $x_3 < 1$, if $t < \tau_N$. However, one may estimate $W(T)$ in Eq. (4) directly by examining the mean-square displacements of inner monomers, $g_1(t)$. As long as these mean-square displacements are smaller than the square of the screening length ξ_{scr} of the excluded volume interactions, which is a few lattice spacings in our model[33], one can use the result[34]

$$g_1(t) \equiv \langle [r_i(t) - r_i(0)]^2 \rangle \sim \langle b^2 \rangle (Wt)^{x_1} \qquad x_1 = [1 + 1/(2\nu)]^{-1} \approx 0.54 \tag{7}$$

where in the last step the exponent $\nu \approx 0.59$ ($\langle R_g^2 \rangle \sim \langle b^2 \rangle N^{2\nu}$ for chains with excluded volume interactions in the dilute limit[70]) was used. Fig. 9 shows mean-square displacements in the bulk of our thin film (using a geometry as in Fig. 1), where fits to Eq. (7) are performed, and the resulting rates $W(T)$ are fitted to a Vogel-Fulcher law (Eq. (5)) or alternatively to Bässler's law[71]

$$W(T) = W(\infty) \exp(-B/T^2) \qquad B = \text{const.} \tag{8}$$

It is seen from Fig. 9 that both Eqs. (5) and (8) fit our data very well, and equally well: We can make no statement about the existence of a "static" glass transition at a nonzero temperature, where the relaxation time then would truly diverge if one could reach that temperature in metastable equilibrium of the supercooled polymer melt. However, our simulation does share this ambiguity of interpretation with experiment on real amorphous materials!

4. Static structure of the "interphase" between the hard walls and the amorphous polymer matrix

In order to model the situation of Fig. 1, we choose a simulation geometry of a $40 \times 40 \times 40$ lattice with periodic boundary conditions only in x and y directions, while in the z-direction instead hard walls are used in the planes at $z = 0$ and $z = 40$. These hard impenetrable walls interact with the effective monomer by excluded volume interactions only, so we focus on the effect of chain confinement only (attractive interactions between monomers and the wall, where chain adsorption at the wall and confinement of chains compete, is considered elsewhere[72]). In all other respects, the model is identical to that of the previous section.

Fig. 10 shows the density profile of all monomers ($\rho_m(z)$) and of the end-monomers ($\rho_{em}(z)$) of the chains, both at a very high temperature ($T = 1.0$) and at a temperature where the slowing down due to the glass transition is already distinctly felt ($T = 0.2$). It is seen that already in the melt far above the glass transition there is an oscillatory density profile. Such oscillatory density profiles near hard walls are well-known from

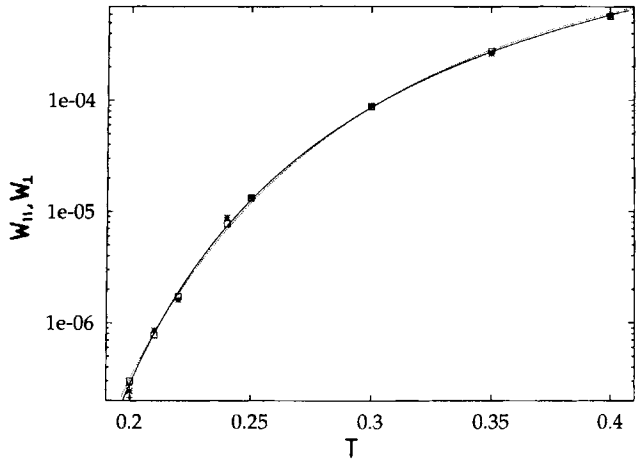

Fig. 9. Temperature dependence of the monomer mobility parallel, $W_{\|}$ (□), and perpendicular, $W_{\perp}$ (*), to the wall for a 40 × 40 × 40 lattice, with two hard walls at z = 0 and z = 40 (cf. Fig. 1), recorded in the bulk region of the amorphous polymer region (i.e., at z = 20) using a volume fraction ϕ = 0.5. Of course, in the bulk the directions parallel and perpendicular to the external walls are equivalent, and hence $W_{\|} = W_{\perp}$. The full line is a fit to the Vogel-Fulcher law, Eq. (5), the dotted line is a fit to Bässler's law, Eq. (8). The temperature T_0 in Eq. (5) resulting from this fit is $T_0 \approx 0.10$ (with a relative accuracy of a few percent). (From Baschnagel and Binder [16])

off-lattice models of simple fluids and polymer chains [18–25], and occur also for rather realistic models including atomistic detail [11]. In contrast, the simplest type of lattice models (i.e., selfavoiding walks on simple lattices [73–77]) do not show this effect. Of course, the details of this layering phenomenon depend both on the local monomeric structure and the energetics of the wall-monomer interaction [11, 17] and hence our model accounts for this oscillating density profile only qualitatively. Nevertheless it is important to incorporate this layering phenomenon at least in a crude way, since the range of these density oscillations is very sensitive on the occurrence of the glass transition, as a comparison between T = 1.0 and T = 0.2 shows (Fig. 10).

Also a comparison between $\rho_m(z)$ and $\rho_{em}(z)$ is interesting: one sees (Fig. 10) that already in the nearly athermal case (T = 1.0) the density of end-monomers also is enhanced near the wall. This is a well-known entropic effect, that has also been already observed in the simulation of many other models as well [11, 19, 22–25, 73, 74, 76]. However, as the temperature is lowered in our model the density of inner monomers gets larger at the wall rather than the density of the end-monomers. This observation can be understood, since the combined effect of the hard wall and of our energy function that favors the bond vector $\boldsymbol{b}$ = (±3, 0, 0) {or permutations thereof} is an alignment of bonds in the groundstate parallel to the wall. This effect leads to a stronger enhancement of the inner monomers than the end-monomers. A comparable inversion of $\rho_m(z = 1)$ and $\rho_{em}(z = 1)$ is not observed in off-lattice simulations of semiflexible

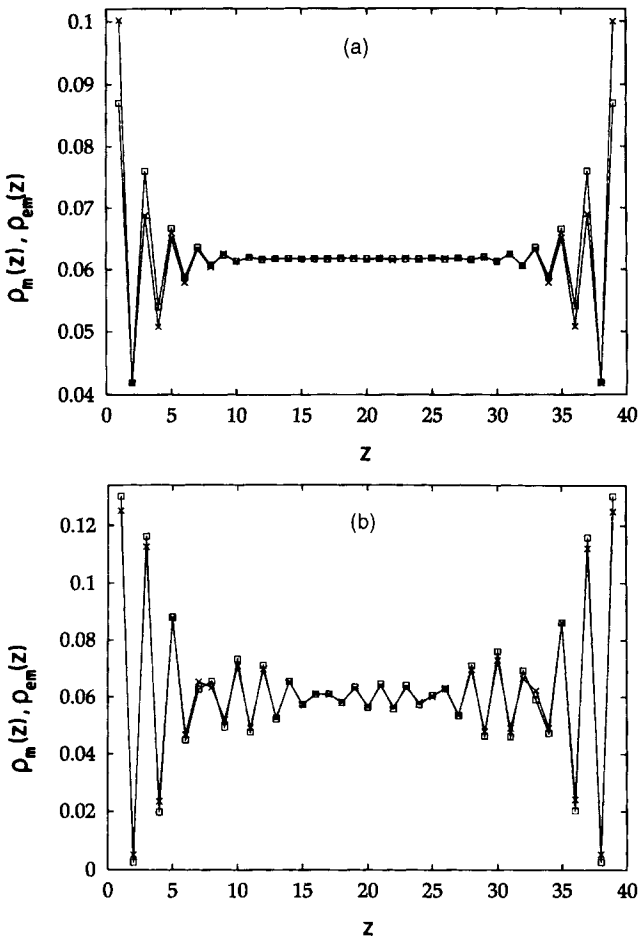

Fig. 10. Comparison of the z-dependence of the monomer density profile $\rho_m(z)$ (□) and the end-monomer profile $\rho_{em}(z)$ (×) at a temperature $T = 1.0$ (a) and a temperature 0.2 (b). Note that $\rho_{em}(z)$ is multiplied by a factor 5, using a chain length $N = 10$, since then in a homogeneous situation chain ends and monomers should all have the density $\rho = \phi/8 \approx 0.0625$. Since the distance between the walls is finite in our geometry (Fig. 1), $D = 40$, and some entropy-driven adsorption at the walls occurs even in the athermal limit, the effective "bulk" density in our simulation is about 0.0615, i.e., $\phi \approx 0.49$ in the bulk. All data are based on an average over 10 independent "replicas" of the same system. (From Baschnagel and Binder[8])

polymer melts with increasing chain stiffness[25], and hence we conclude that such details are controlled by specific properties of the model (or the real polymer material, respectively). Of course, such properties are very sensitive to a difference in interaction

between the wall and end-monomers compared to the interaction between the wall and inner monomers[76], which is rather natural to assume due to their different chemical structure.

We feel, however, that a much more fundamental effect is the pronounced increase of the *range* of these density oscillations near the wall, when the glass transition is approached. The decay length of these density oscillations can be interpreted as a measure for the thickness of the interphase region in Fig. 1.

In order to quantify this idea, it is convenient to proceed as follows[8]. Since the density profiles are symmetric around the middle of the simulation box, both halves are combined to an average profile $\bar{\rho}_m(z)$ (or $\bar{\rho}_{em}(z)$, respectively). We then define an excess probability to find a monomer at position z by $p_m(z)$,

$$p_m(z) = | \bar{\rho}_m(z) - \rho_m^{bulk} | / \sum_{z=1}^{L/2} | \bar{\rho}_m(z) - \rho_m^{bulk} | \tag{9}$$

ρ_m^{bulk} being the average of $\rho_m(z)$ from $z = 15$ to $z = 25$. We then define a "correlation length"

$$\xi_m = \sum_{z=1}^{L/2} z p_m(z) \tag{10}$$

Similarly a length ξ_{em} can be defined[8] from an analogous procedure for the end-monomer profile, and a length ξ_{em} from the "chain monomer profile" $N_{cm}(z)$, defined[20] as the average number of monomers in layer z that belong to the same chain. The temperature dependence of these various lengths is shown in Fig. 11, comparing it to that of the bulk gyration radius. At high temperatures, all lengths ξ_m, ξ_{em} and ξ_{cm} are clearly smaller than the gyration radius. We expect that the order of magnitude of these lengths is only the same because our chain length is so short ($N = 10$) — in fact, while the bulk gyration radius R_g^{bulk} increases with chain length, $R_g^{bulk} \sim b\sqrt{N}$, the other lengths should remain of the order of an average bond length b^{bulk} (≈ 2.6 lattice spacings in our model), which is the characteristic length for local density variations in a dense polymer system. Therefore it is of great interest to note from Fig. 11 that the lengths ξ_m, ξ_{em} and ξ_{cm} all increase dramatically with decreasing temperature at low temperatures, and for $T \leq 0.2$ are already larger than R_g^{bulk}. Unfortunately, the large statistical error bars preclude us still from making any statements whether these lengths diverge to infinity, as the temperature is still lowered further — the controversial issue whether the glass transition is linked to a diverging lengthscale[78-80] hence remains outside of consideration here.

It is also an interesting question to ask to what extent the surface of the fibers orients the adjacent polymer coils as a whole. To study this question, profiles of the parallel part $\{R_{g\parallel}(z)\}$ and the perpendicular part $\{R_{g\perp}(z)\}$ of the mean-square gyration radius of chains with center of mass in the plane z are recorded (Fig. 12)[8]. Remember that the instantaneous configuration of a random Gaussian coil is not a spherical object, but rather a diffuse soap-shaped object, with three fairly different components of the gyration tensor. In the bulk, the axes along the three directions characterizing this tensor are randomly oriented, and on the average the spherical symmetry is respected

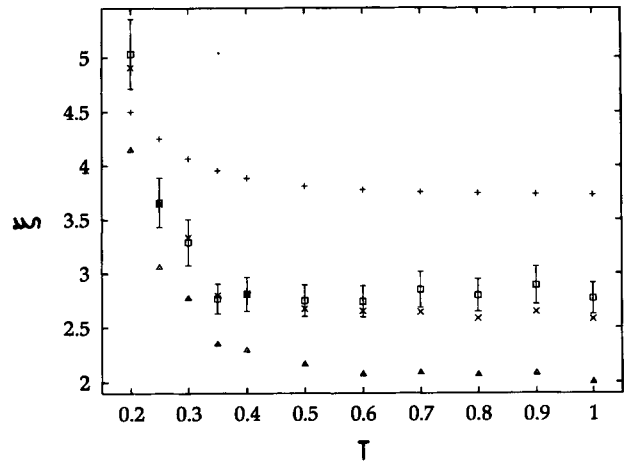

Fig. 11. Characteristic lengths for the effect of a hard wall on a polymer melt plotted versus normalized temperature: decay length ξ_m (×), and the chain-monomer profile ξ_{cm} (△). Additionally, the bulk value of the radius of gyration $R_g^{bulk} = (\langle R_{g\parallel}^2 \rangle + \langle R_{g\perp}^2 \rangle)^{1/2}$ (+) is shown for comparison. R_g^{bulk} is the average value of $R_g(z)$ for $15 \leq z \leq 25$. (From Baschnagel and Binder[8])

then, $\langle R_{gx}^2 \rangle = \langle R_{gy}^2 \rangle = \langle R_{gz}^2 \rangle = \langle R_g^2 \rangle/3$. If the chain comes close to a wall, the repulsive interaction with the wall constrains the possible configurations of the coil, and then there is a tendency to orient the longest axis of the "soap-shaped" coil parallel to the wall, and the shortest axis perpendicular to it. Therefore $\langle R_{g\parallel}^2 \rangle$ strongly increases, when the center of mass position of the coil is close to a wall, and $\langle R_{g\perp}^2 \rangle$ decreases at the same time. This orientation effect occurs already far above the glass transition (Fig. 12a), but gets far more pronounced for temperatures near the glass transition (Fig. 12b).

While the effect seen in Fig. 12a, namely an orientation of the coil on the scale of its own gyration radius, is intuitively obvious and expected from other simulations[19–23,76], the large range over which the walls at $T = 0.2$ have an orienting effect (Fig. 12b) is rather unexpected: it means that chains are still affected which are too far from the wall to interact with it directly, they feel the wall only indirectly through structural correlations with neighboring chains closer nearby the wall.

This phenomenon has been examined further by checking whether the decrease of $R_{g\perp}^2(z)$ near the wall scales with the bulk gyration radius of the chain (Fig. 13). For athermal melts (where the bulk gyration radius $R \equiv R_g^{bulk}/\sqrt{3}$ can be varied by varying the chain length, of course) this scaling property is reasonably well fulfilled[76], $R_{g\perp}^2(z)/R^2$ plotted vs. z/R yields a universal curve, independent of N, see Fig. (13a). For the present model of a glassy system, however, an analogous scaling property does not hold for the data at low temperatures ($T \leq 0.3$). Thus obviously the bulk correlation length R is not the characteristic length that controls the chain orientation effect due to walls near the glass transition.

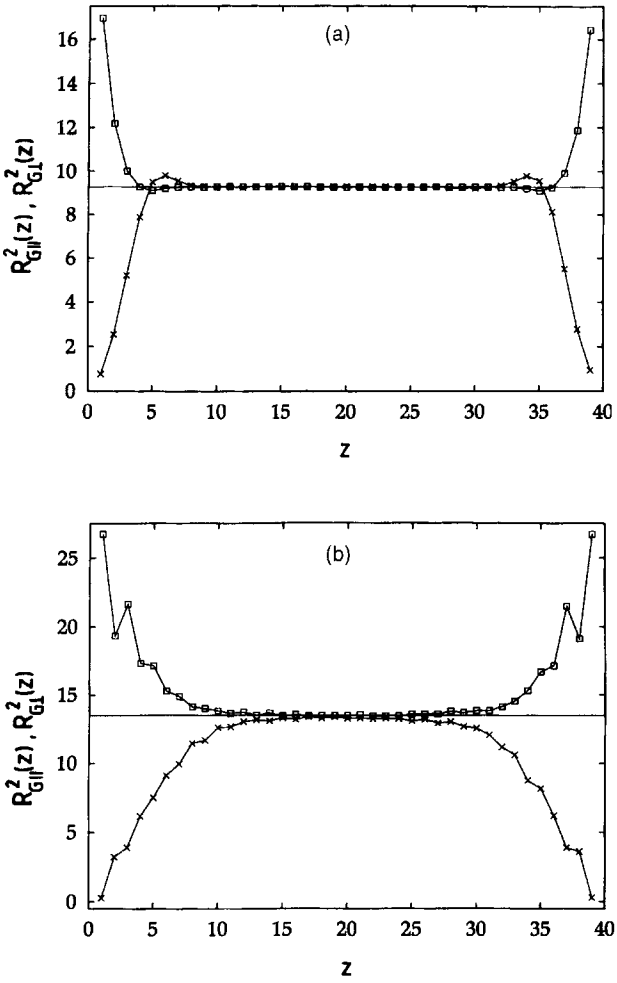

Fig. 12. Plot of the distance profile of the component of the radius of gyration parallel to the wall ($R^2_{g||} = \langle R^2_{gx}\rangle + \langle R^2_{gy}\rangle$) and perpendicular to the wall ($R^2_{g\perp} = 2\langle R^2_{gz}\rangle$), for the normalized temperature $T = 1.0$ (a) and 0.2 (b). The horizontal straight line shows corresponding bulk values. (From Baschnagel and Binder[8])

Gratifyingly, a reasonable scaling behavior is found if the monomer correlation length ξ_m is taken as the characteristic length to rescale the profile of $R^2_{g\perp}(z)$, see Fig. 13c. Thus there is a well-defined thickness ξ_m of the "interphase", the region where the structural arrangement of the chains is affected by the surface. Thus, the results described in this section indicate that in the glassy state of a composite material there is a region of mesoscopic extent (i.e., several nanometers) adjacent to the fiber-matrix interface, where physical properties are distinctly anisotropic. Since it is very difficult

to equilibrate supercooled polymer melts near the glass transition temperature T_g in the framework of computer simulations[53], it is very difficult to estimate the thickness of this region more precisely. Simulations based on extremely rapid quenching of a high-temperature fluid very likely freeze in the uncorrelated structure of the fluid and then would miss (or at least underestimate) this effect. Clearly, there is need to quantify this phenomenon more precisely, and to explore its consequences on physical properties of the material — the studies reviewed here should be viewed as a first step only.

5. Anisotropic motions in supercooled polymer melts near a hard wall

Since the density in a polymer melt has a very direct consequence on the monomeric mobility (the higher the density, the smaller the mobility), one expects that the oscillatory density profile near hard walls has an immediate consequence on the mobility as well. This idea is already borne out by the acceptance rate of the monomer moves (Fig. 14). It is seen that the acceptance rate for moves parallel to the wall is not much affected even for temperatures close to the glass transition: this is a first indication that the structure in the "interphase" forms in such a way that motions parallel to the flat hard wall are relatively easily possible[16]. Of course, the acceptance rate of the moves is not really sensitive to the occurrence of the glass transition, since motions where monomers jump back and forth in "cages" formed by their environment are also counted as "successful moves", although they do not contribute to structural relaxation[47, 48, 52, 53].

A better description of monomeric motions in a layer z above the wall is possible when one considers the time-dependent mean-square displacements of the monomers. We define z-dependent mean-square displacements of inner monomers in directions parallel and perpendicular to the walls by

$$g_{1\,\parallel}(z, t) = \langle [x_i(t) - x_i(0)]^2 + [y_i(t) - y_i(0)]^2 \rangle \tag{11}$$

$$g_{1\,\perp}(z, t) = \langle [z_i(t) - z_i(0)]^2 \rangle \qquad z \equiv z_i(0) \tag{12}$$

which characterize the local motion of all monomers originally situated at layer z at time $t = 0$[16]. Similarly, we also consider displacements of inner monomers in the reference frame of the center of mass of the considered chain, $g_{2\,\parallel}(z, t)$ and $g_{2\,\perp}(z, t)$, and of the center of mass itself,

$$g_{3\,\parallel}(z, t) = \langle [x_{cm}(t) - x_{cm}(0)]^2 + [y_{cm}(t) - y_{cm}(0)]^2 \rangle \tag{13}$$

$$g_{3\,\perp}(z, t) = \langle [z_{cm}(t) - z_{cm}(0)]^2 \rangle \qquad z \equiv z_{cm}(0) \tag{14}$$

Fig. 15 shows selected typical data for these displacements. At high temperatures and in the bulk of the film, away from the hard walls (Fig. 15a), we recover the standard behavior well-known for Rouse dynamics[34, 35, 61, 62]: for short times where the mean-square displacements of inner monomers are smaller than the screening length of excluded volume interactions we have Eq. (7), i.e.

$$g_{1\,\parallel}(z, t) \sim g_{2\,\parallel}(z, t) \sim \langle b^2 \rangle (Wt)^{x_1} \qquad x_1 = 1/[1 + 1/(2\nu)] \approx 0.54 \tag{15}$$

where in the last step the exponent $\nu \approx 0.59$ for the three-dimensional self-avoiding walks was used[70]. In the bulk of the film, the mean-square displacements for $z = 15$ (symbols in Fig. 15a, b) and $z = 25$ (lines in Fig. 15a, b) coincide, illustrating that neither $\langle b^2 \rangle$ nor W depend on the position z, as expected. Already at $g(t) \approx 1$, the screening of excluded volume starts to be gradually felt, and then a crossover occurs to the Rouse behavior for simple Gaussian chains, $g_{1\parallel}(z, t) \sim g_{2\parallel}(z, t) \sim t^{1/2}$. This behavior continues up to the Rouse time τ_{Rouse}, which scales as

$$\tau_{\text{Rouse}} \sim W^{-1} N^2 \tag{16}$$

For $t > \tau_{\text{Rouse}}$, the mean-square displacement in the center of mass system crosses over to a saturation value which is nothing but the corresponding mean-square gyration

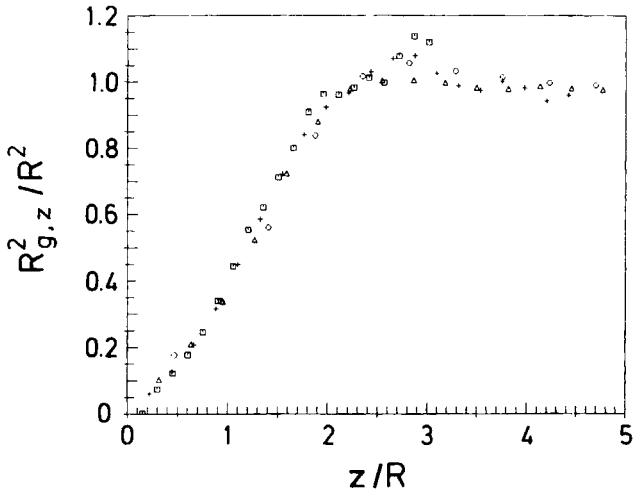

Fig. 13.a.

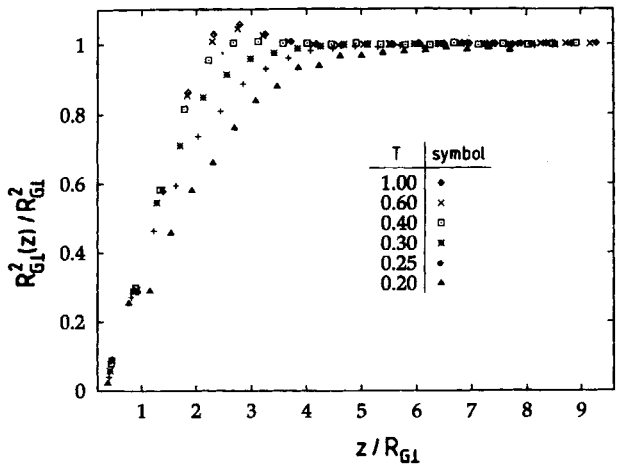

Fig. 13.b.

Fig. 13.c.

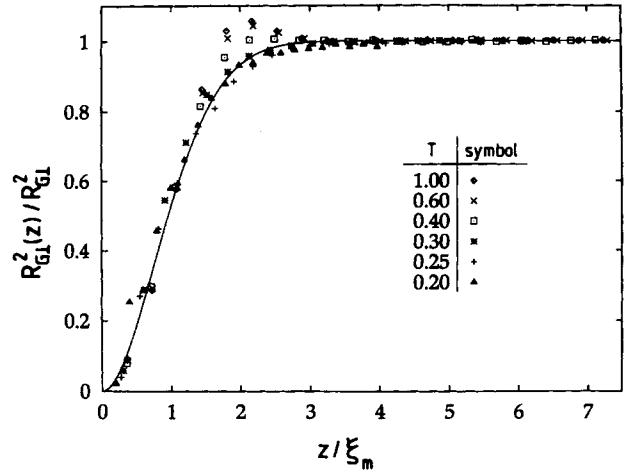

Fig. 13. (a) Scaling of the perpendicular component. $R^2_{g\perp}(z)$ of the mean-square radius of gyration of self-avoiding walks in an athermal melt as a function of the distance z of the chain center of mass from a repulsive wall. All lengths are normalized by $R = R_g^{bulk}/\sqrt{3}$. The symbols denote chain lengths $N = 10$ (circles), 20 (triangles), 40 (crosses) and 80 (squares). (From Wang and Binder[76].) (b) Plot of $R^2_{g\perp}(z)/R^2_{g\perp}$ versus $z/R_{g\perp}$ for the bond fluctuation model for various representative temperatures, as shown in the figure. $R_{g\perp}$ ($=R$ of Fig. 13a) is the bulk value of the gyration radius component. (c) Same as (b) plotted versus z/ξ_m. (From Baschnagel and Binder[8])

radius component, while $g_{1\parallel}(z, t)$ starts to join the center of mass mean-square displacement $g_{3\parallel}(z, t)$, which simply follows an Einstein relation

$$g_{3\parallel}(z, t) = 4D_{\parallel} t \qquad t \geq \tau_{\text{Rouse}} \tag{17}$$

Note that the factor 4 in Eq. (17) results simply, since we consider quasi-twodimensional motions in x, y directions parallel to the walls. While in the simple Rouse model[61,62] Eq. (17) applies already for times larger than the monomeric reorientation time W^{-1}, in the dense polymer systems Monte Carlo calculations show[34,35,57] that there exists a regime where anomalous diffisuion occurs, with $g_3(t) \sim t^{x_3}$, $x_3 \approx 0.8$, for $W^{-1} \leq t \leq \tau_{\text{Rouse}}$, for chains that are short enough such that entanglement effects can be neglected. This behavior is outside of consideration here, however.

At low temperatures (Fig. 15b) the behavior is similar, with the exception that there exists an intermediate regime of times where the increase of mean-square displacements with time is anomalously slow. This slowing down is due to the fact that the monomeric motions are strongly hindered by their neighbors: bonds in the environment already are in the groundstate and have to leave it again to allow for further motion. In other words, structural relaxation is needed to release the monomers from the "cages" formed by their environment. As a consequence, it is very difficult to follow these displacements over large enough times such that one can see the simple diffusion behavior (Eq. (17)) at low temperatures. In fact, the time regime displayed in Fig. 15b

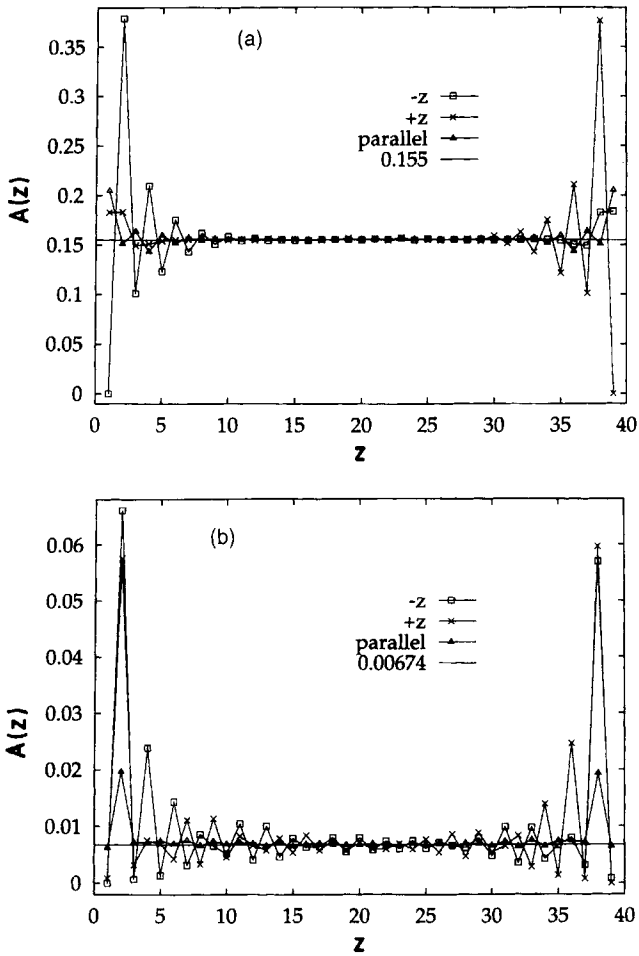

Fig. 14. Profile of the acceptance rate $A(z)$ at $T = 1.0$ (a) and $T = 0.18$ (b) plotted vs. the distance z of the monomer from the wall. Moves in perpendicular direction ($-z$: □; $+z$: ×) and parallel to the wall (△) are distinguished. The horizontal straight line indicates the bulk value of the acceptance rate, which was determined as the average of $A(z)$ in the range $15 \leq z \leq 25$. (From Baschnagel and Binder[16])

is not long enough to see the crossover to Eq. (17) yet, $R_{g\parallel}^2$ is beyond the scale of this plot, and thus neither τ_{Rouse} nor $D_\parallel$ can be estimated directly.

On the other hand, in the early time regime one can still use Eq. (15) to estimate the rate W. This is also true for the monomeric displacements close to the surface (Fig. 15c). While the decrease of the diffusion constant $D_\parallel$ can thus be followed only over two decades, the rates $W_\parallel$, $W_\perp$ for monomeric mean-square displacements parallel and perpendicular to the wall could be obtained for more than three decades (Fig. 16).

Since the analysis of $W_{\parallel}$, $W_{\perp}$ thus spans a larger temperature range than that of $D_{\parallel}$, it is no surprise that the Vogel-Fulcher temperatures extracted from the various fits are not in good mutual agreement with each other: it is now also clearly established experimentally[69] that the Vogel-Fulcher law is not in perfect agreement with the data on relaxation times, and that the resulting Vogel-Fulcher temperature sensitively depends on the temperature region included in the fit. But a key result of our study is already obvious qualitatively from Fig. 16b: the mobility for lateral motions of monomers adjacent to the planar wall is much higher than the mobility for perpendicular motions. This enhancement of the mobility becomes rather dramatic near the glass transition. While such an effect, of course, would be expected for the "free" surface of an amorphous polymer against vacuum or air, because there the monomers can relax more freely than they could in the bulk, it is unexpected for the interface between polymers and hard walls. In our model, it can be explained because effective bonds that reach their ground state can pack relatively easily adjacent to the hard wall, and thus there is less "geometric frustration" in the interfacial region than there is in the bulk.

We emphasize, however, that we do not expect that this facilitated motion of monomers near hard repulsive walls is a universal phenomenon, rather we consider it as a peculiarity of our simplified model. In real materials, we consider it rather likely that instead the motions of monomers parallel to a wall are hindered due to a variety of effects — misfit of chemical groups of a monomer with the atomistic corrugation of the solid wall, binding forces monomer-wall of various types, and — last but not least — mesoscopic heterogeneity of the wall due to chemisorbed impurities, surface roughness, etc. It is hard to incorporate all these phenomena into a valid model description, and clearly a precise experimental characterization of the fiber surface that is used is mandatory. While our model implies that "locally" the glass transition temperature of the interphase is lowered, and consequently in a thin film geometry the glass transition temperature of the whole film would be lower than that of a bulk sample, it may seem more natural to expect that surface heterogeneity might cause an effect in the opposite direction — although reports can be found in the literature[10] which show that for some types of walls T_g is raised and for other types of walls it is lowered, as in our study. Thus the effect of fiber surfaces on the dynamics of polymers in the interphase region is clearly expected to be of non-universal character, and our modeling has captured some ingredients (mostly of entropic origin) of this interesting behavior only.

6. First steps towards the modeling of fiber-matrix interfaces under shear

Measuring the response of a thin polymeric film confined between two plates against shear deformations is a very significant experimental tool to elucidate many properties of the film, which are important for applications[16]. Remember that mechanical properties of composite materials are to a large extent controlled by the forces transmitted across the interfaces between fibers and the amorphous polymer matrix[1-7], and such shear experiments[15] can model this situation and thus yield insight in the resulting physical behavior at least on a semi-microscopic scale. Of

course, the interpretation of such experiments in terms of atomistic concepts about the structure and dynamics of the polymer coils in the amorphous matrix can only be rather indirect, and it is this aspect where computer simulation should help, providing a motivation for the present section.

In principle, the proper simulation technique to study responses against shear deformation is nonequilibrium molecular dynamics (NEMD)[81,82]. While this technique is well established for simple liquids[81], it has only been developed recently for polymeric systems[82], and an application near the glass transition of a polymer melt seems difficult.

Therefore we have applied an approximate Monte Carlo method, similar in spirit to a recent study of polymer brushes under shear[43], which we consider rather successful. There the effect of the shear flow was simply modeled in a Monte Carlo framework by postulating an asymmetry in the jump rate p_{+x} (in the direction of the flow) as compared to the jump rate p_{-x} (in the direction against the flow). Motivated by the

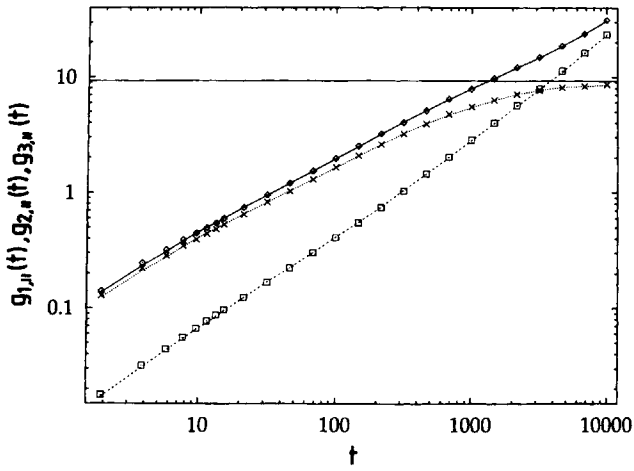

Fig. 15.a.

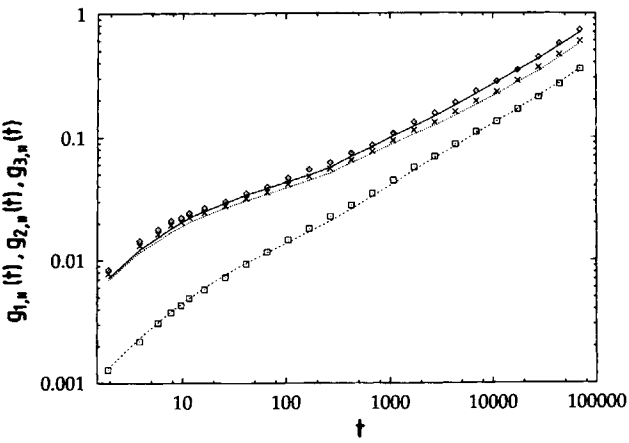

Fig. 15.b.

Fig. 15. c.

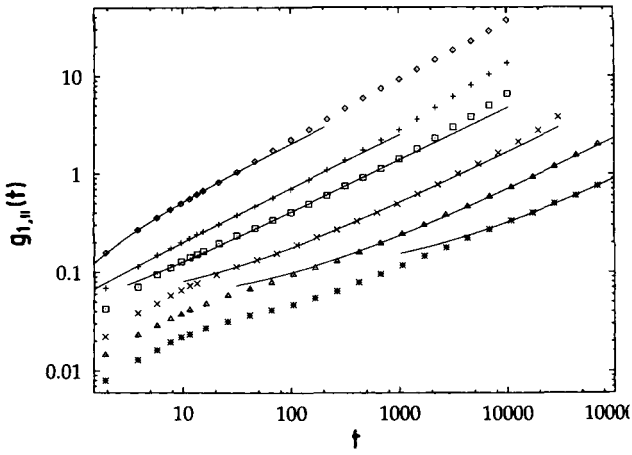

Fig. 15. (a) Time dependence of the parallel component of various mean-square displacements at $T = 1.0$ in the bulk of the film ($z = 15$: symbols; $z = 25$: lines): $g_{1\parallel}(z, t)$ ($\diamond$), $g_{2\parallel}(z, t)$ ($\times$) and $g_{3\parallel}(z, t)$ ($\square$). The horizontal line is the bulk value of the parallel component of the gyration radius square, at which $g_{2\parallel}(z, t \to \infty)$ saturates. (b) Same as (a) but for $T = 0.2$. (c) Temperature dependence of $g_{1\parallel}(z = 1, t)$ for various temperatures, $T = 0.2$ ($*$), 0.22 ($\triangle$), 0.25 ($\times$), 0.3 ($\square$), 0.35 ($+$) and 1.0 ($\diamond$). Solid lines are fits to the law $g_{1\parallel}(z, t) = b_{\parallel}^2(z)[W_{\parallel}(z)t]^{0.54}$ from which $W_{\parallel}(z)$ is extracted since $b_{\parallel}(z)$ is estimated independently[8]. (From Baschnagel and Binder[16])

principle of detailed balance, we introduce a parameter p such that $p_{+x} = p/(6N(p))$ and $p_{-x} = 1/(6pN(p))$, where $N(p)$ is a normalization constant for the jump probabilities. Requiring $\sum_i p_i = 1$, one obtains

$$p_{+x} = \frac{p^2}{p^2 + 4p + 1}, \quad p_{-x} = \frac{1}{p^2 + 4p + 1}, \quad p_{\pm y} = p_{\pm z} = \frac{p}{p^2 + 4p + 1} \tag{18}$$

The so-defined jump probabilities have the following properties: (1) If $p = 1$, the no-shear case $p_{\pm x} = p_{\pm y} = p_{\pm z} = 1/6$ is recovered. (2) For $p \to \infty$, all motion except that in direction of the shear force (i.e., $+x$ direction) ceases. (3) For small p, the difference $p_{+x} - p_{-x}$ which is proportional to the shear rate, becomes $p_{+x} - p_{-x} \approx (p - 1)/3$. Since in dense polymer melts hydrodynamic forces are screened off on very short distances (the hydrodynamic screening length is of the same order as the screening length for the excluded volume forces[83]), we apply Eq. (18) in the first layer adjacent to the wall only, assuming that the direct effect of the shear forces due to the wall will be screened off further away from the surface. Of course, due to the interactions among the polymer chains the interior layers will be indirectly affected, and the resulting response of the "interphase" to the shear is the topic of interest here.

Due to our periodic boundary conditions in the x and y directions, it is clear that Eq. (18) leads to a kind of steady state situation with a flow of monomers (and polymers) in the $+x$-direction. Although this nonequilibrium steady state situation is a far from

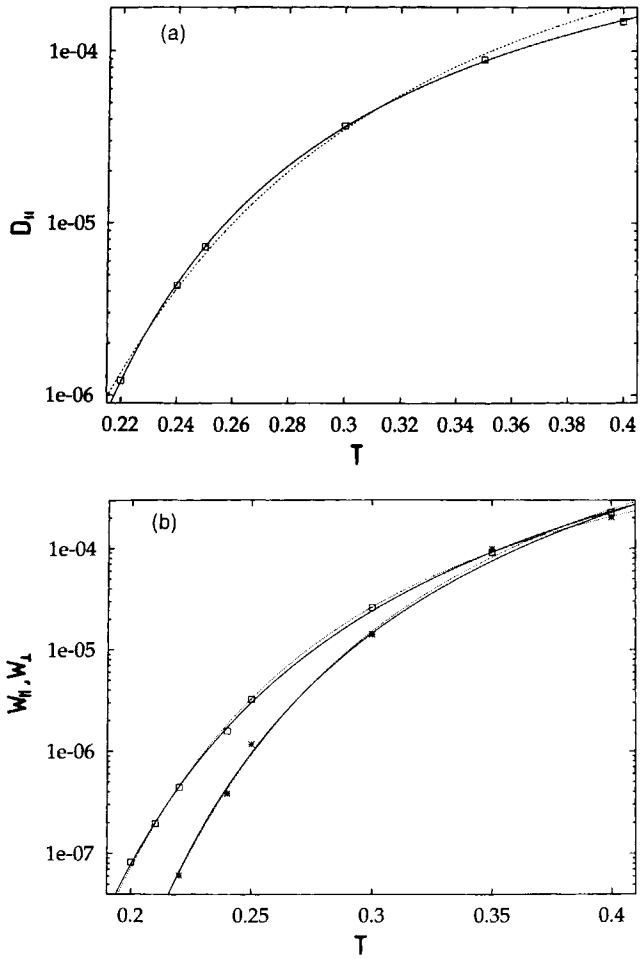

Fig. 16. (a) Temperature dependence of the average diffusion constant $D_{||}$ in the film (averaged over all polymers irrespective of their position). The straight line is a fit to the Vogel-Fulcher law, Eq. (3), while the dotted line is a fit to Bässler's law, Eq. (8). The Vogel-Fulcher temperature T_0 resulting from $D_{||}$ would be $T_0 \approx 0.13$. (b) Temperature dependence of the rates $W_{||}$ (□) and $W_{\perp}$ (*) for monomeric motions in the plane $z = 1$ adjacent to the wall. Again dotted lines are fits to Bässler's law, Eq. (8), and full lines fits to the Vogel-Fulcher law, Eq. (5). The resulting Vogel-Fulcher temperatures are $T_0 = 0.10$ ($W_{\perp}$) and $T_0 = 0.07$ ($W_{||}$), respectively. (From Baschnagel and Binder [16])

equilibrium state, one can nevertheless study "static properties" (Fig. 17). It is interesting to note that the shear deformation strongly enhances the layering effect caused by the hard wall (Fig. 17a). Also the chain configurations get strongly distorted, the parallel component is much larger near the wall (Fig. 17b) than without shear: compare

the enhancement on the sheared wall ($z = 40$) with the enhancement on the wall that stays at rest ($z = 0$). Thus the chains are strongly stretched in the direction of the flow. A similar effect has also been detected for polymer brushes in shear flow[43].

It is interesting to note that nevertheless the perpendicular component (Fig. 17c) is not much affected very close to the wall. But unexpectedly, a rather pronounced maximum occurs in the profile of $R^2_{g\perp}(z)$ near $z \approx 34$, which is at a distance where the chains no longer interact directly with the wall. A small precursor of such a maximum does also occur at a wall at rest (near $z \approx 6$), and probably these structures both reflect correlation effects between the polymer chains: while the layer of coils rather adjacent to the walls is oriented with the long axis of their gyration tensor parallel to the wall, this orientation induces an opposite orientation of the next layer of coils. Thus, we interpret this phenomenon as a "layering" in the orientation of coils, qualitatively similar to the layering of the density: but while the scale for the density oscillations is the lattice spacing in our model, the scale for the layering chain orientation is the gyration radius of the chains itself (remember the scaling properties of the profile for $R^2_{g\perp}(z)$ discussed in section 4 for the athermal case).

It is also interesting to consider the profile of the acceptance rate $A(z)$, where we now distinguish moves in all 6 directions of the simple cubic lattice (Fig. 18). Fig. 18 compares the behavior of $A(z)$ at the wall at rest ($z = 0$) with that at the wall where the shear force ($p = 2$) is applied ($z = 40$). The application of shear has two consequences: On the one hand, the jump rates in virtually all directions (except the $+z$-direction towards the sheared wall at larger distances, i.e., $z = 30, 32, 34, 36$) are distincly reduced in the layers affected by the shear, as compared to the corresponding $A(z)$-values at the non-moving wall and to the bulk acceptance rate. This means that the chains near the sheared wall take configurations which are rather immobile, requiring jumps against the shear flow to re-arrange them. The shear flow hence causes a stiffening of the interfacial region, in our model. On the other hand, the shear force extends the range over which the perturbation induced by the wall penetrates into the bulk. Except for the jump direction towards the wall $A(z)$ becomes isotropic at $z \approx 5$ for the wall at rest, i.e., on the length scale of a bond, whereas the bulk acceptance rate is reached only at $z \approx 31$ for the sheared wall, i.e., on the length scale of the gyration radius. This extension of the penetration depth (i.e., of the size of the interphase) is not visible in the profiles of the static properties of Fig. 17, from which one could conclude that the influence of the shear force is only to render all present effects more pronounced without increasing the size of the interphase. The comparison of Figs. 17 and 18 therefore suggests that the size of the interphase cannot be unambiguously determined based on static properties only in the presence of shear. It would therefore be interesting to check whether this conclusion holds up under scrutiny when the monomer mobilities $W_{\parallel}$ and $W_{\perp}$ are studied instead of A.

Finally we turn to the velocity response of our model to the shear forces. It turns out that this is an extremely difficult problem, because it takes a very long time until a steady state flow field is reached (Fig. 19: $p = 2$). Immediately after the flow field is switched on ("not aged" curves in Fig. 19), one finds rather large displacements, because those monomers that contribute to the structural rearrangement of the chains (chain stretching, cf. Fig. 17) contribute initially to the mean displacement also.

However, this relaxation process towards the steady state configurations should not be included in the measurement of the mean displacement during the steady state flow, as Fig. 19 shows ("aged curves" in Fig. 19). For $p = 3$ smaller steady state displacements were found than for $p = 2$, indicating that for strong shear rates chains are locked in configurations from which they can escape only via crossing high entropic barriers in phase space. These data hence indicate that the choices $p = 2, 3$ discussed here already are in a regime where the response to the shear stress is highly nonlinear. The increase of $\langle x_{cm}(t) \rangle$ in Fig. 19 corresponds to an average velocity of $v \approx 3.3 \cdot 10^{-5}$ (in units of inverse Monte Carlo steps per monomer), and noting that the relaxation time is of the order of $\tau \approx 3000$ Monte Carlo steps, we note $v\tau \approx 10^{-1}$ here, which is not unreasonable.

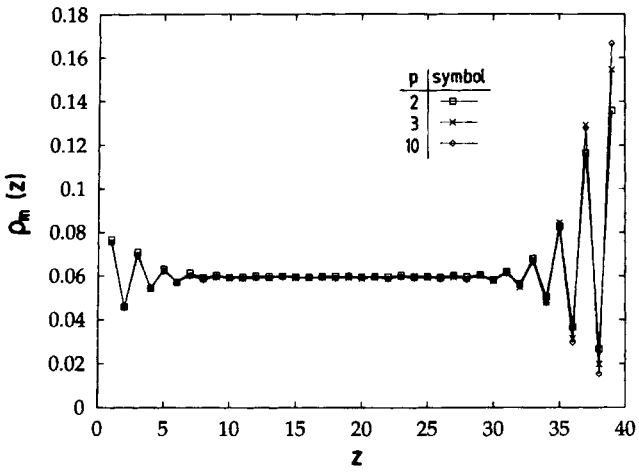

Fig. 17.a.

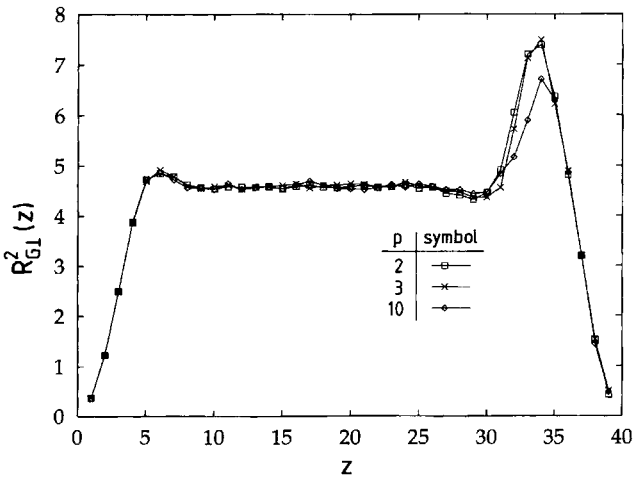

Fig. 17.b.

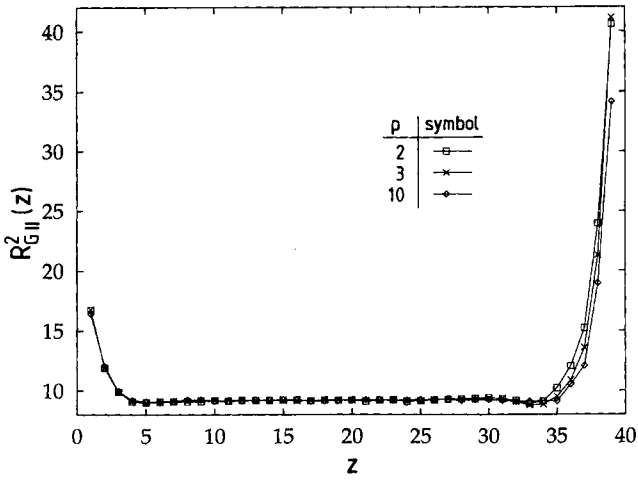

Fig. 17. c.

Fig. 17. (a) Monomer density profile for an athermal polymer melt ($T \to \infty$) for different shear rates applied in the plane $z = 39$, while the wall at $z = 0$ stays at rest. The shear rate increases with p (see Eq. (18) and the corresponding discussion in the text). (b) Profile of the perpendicular part $R^2_{g\perp}(z)$ of the mean-square gyration radius, for the same situation as in (a). (c) Same as (b) but for the parallel part $R^2_{g\parallel}(z)$

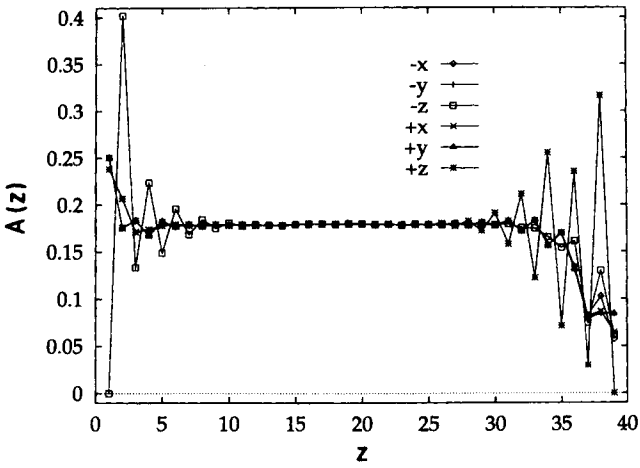

Fig. 18. Profile of the acceptance rates $A(z)$ for moves in the 6 lattice directions of the simple cubic lattice, for an athermal melt ($T \to \infty$) and $p = 2$

7. Discussion and outlook

In the present paper, a model was developed to describe the interfacial region between supercooled polymer melts (and the resulting amorphous materials resulting from

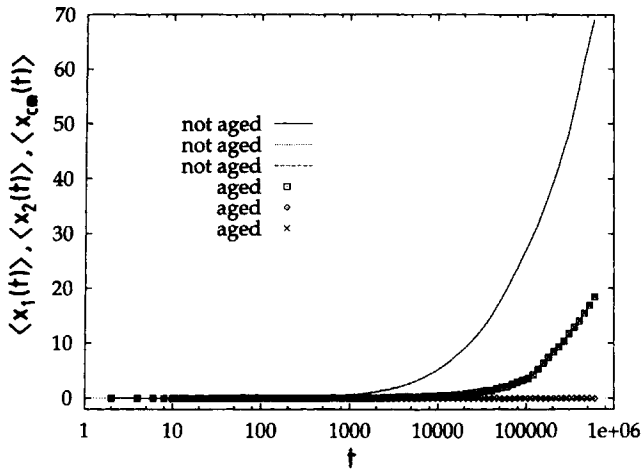

Fig. 19. Time-dependent mean displacement $\langle x_1(t)\rangle$ of inner monomers (solid line, □), $\langle x_2(t)\rangle \equiv \langle x_1(t) - x_{cm}(t)\rangle$ of inner monomers in the center of gravity systems of the chain (dotted line, (◇), and $\langle x_{cm}(t)\rangle$ of the center of mass (dashed line, ×) in the system, averaged over all layers of the system. Note that in the steady state $\langle x_2(t)\rangle \equiv 0$, as observed for systems that are aged over $6 \cdot 10^5$ Monte Carlo steps per monomer. Curves show data that are not aged at all (i. e., the shear flow is switched on at time $t = 0$ and immediately mean displacements are measured). Data again refer to the choice $p = 2$

quenches below the glass transition temperature) and hard walls. This approach uses the bond fluctuation model with a Hamiltonian depending on the bond length only, and the walls are treated as structureless and purely repulsive. Already in earlier work it had been shown that the bond fluctuation model can describe the qualitative features of the glass transition of supercooled polymer melts in the bulk rather nicely, and thus we feel that it is legitimate to study effects due to constraining interfaces in the framework of this simple model, too. Of course, it is clear that rather different properties are expected locally near the interface, depending on the precise nature of the interactions between the monomer and the wall. However, the range over which these interfacial effects spread out into the bulk is a much more universal property, and thus we believe that the observation of a characteristic length ξ_m over which the "interphase" adjacent to the wall significantly differs from the bulk is a general feature, which is not simply a consequence of too restrictive model assumptions, but carries over to real polymer melts.

This characteristic length ξ_m strongly increases as the temperature is lowered; it is tempting to speculate that ξ_m would diverge to infinity at the static glass transition temperature, if such a temperature exists. However, the strong slowing down of structural relaxation makes it impossible to come very close to such a temperature, and hence we cannot attempt to locate such a static glass transition even for our simplified model. Also the precise nature of the long range structural correlations that develop (and which we measure only indirectly via these wall effects) remains obscure. But this

structural anisotropy that develops near the wall also has a subtle influence on dynamic properties. In our model, the hard wall reduces the "geometric frustration" for effective bonds adjacent to the wall, thus facilitating their motion, and leading to a lowering of the glass transition temperature in confined thin films. However, it is conceivable that different model assumptions about wall-monomer interactions could lead to the opposite effect. A study of this case, however, was beyond the scope of the present paper.

A practically very important question about interfaces in amorphous materials (such as occur at the fiber surfaces embedded in amorphous polymer matrices) is the response under shear deformation. While we have shown that also this problem is to some extent accessible to simulation, our results mostly have the character of a feasibility study. Nevertheless, they indicate the existence of physically interesting effects. The application of shear forces strongly enhances the perturbations on the chains' structure, which a hard wall at rest already induces. The monomer density at the wall increases, and the chains in direct contact to the sheared wall become strongly oriented parallel to it, which in turn leads to a preferential perpendicular orientation of chains further away from the wall. Despite this influence the shear force does not seem to affect the size of the interphase as long as profiles of static quantities are considered only. An analysis of the spatial dependence of the acceptance profile, however, indicated that shear might increase the size of the interfacial region. Whether these findings are mere consequences of the applied model and the simulation technique, remains unanswered at present. Again the interesting question on how this behavior is affected by different assumptions on the wall-monomer interactions has not yet been touched. It is clear that the present model study is a first step only, and one of its main purposes has been to stimulate corresponding experiments and simulations. In particular, an extension of the present study to off-lattice models (such as those of ref. [84]) would be very interesting.

This research was supported by the *Bundesministerium für Bildung, Wissenschaft, Forschung und Technologie (BMBF)* under grant number 03M4076A3. We thank *J. Klein, W. Paul* and *M. Wolfgardt* for helpful and stimulating discussions.

[1] G. M. Newaz, in *"Materials Science and Technology"*, Vol. 13, T. W. Chou, Ed., VCH Publ., Weinheim 1993
[2] H. Ishida, P. Bussi, in *"Materials Science and Technology"*, Vol. 13, T. W. Chou, Ed., VCH Publ., Weinheim 1993
[3] M. V. Gandhi, B. S. Thompson, *"Smart Materials and Structures"*, Chapman & Hall, London 1992
[4] D. R. Lovell, *"Carbon and High-Performance Fibres Directory"*, Chapman & Hall, London 1991
[5] D. Wolf, S. Yip, Eds., *"Materials Interfaces: Atomic-level Structure and Properties"*, Chapman & Hall, London 1991
[6] H. M. Flower, *"High-Performance Materials in Aerospace"*, Chapman & Hall, London 1992

[7] L. T. Drzal, *Adv. Polym. Sci.* **75**, 1 (1985)
[8] J. Baschnagel, K. Binder, *Macromolecules* **28**, 6808 (1995)
[9] G. Krausch, *Mater. Sci. Eng., R:* **14**, 1 (1995)
[10] J. L. Keddie, R. A. L. Jones, R. A. Cory, *Europhys. Lett.* **27**, 59 (1994); *Faraday Discuss.* **98**, 219 (1994)
[11] D. Y. Yoon, M. Vacatello, G. D. Smith, in *"Monte Carlo and Molecular Dynamics Simulations in Polymer Science"*, K. Binder, Ed., Oxford University Press, Oxford and New York 1995, Chap. 8
[12] A. N. Semenov, J.-F. Joanny, *Europhys. Lett.* **29**, 279 (1995); *J. Phys. (France) II* **5**, 859 (1995)
[13] G. J. Fleer, M. A. Cohen Stuart, J. M. H. M. Scheutjens, T. Cosgrove, B. Vincent, *"Polymers at Interfaces"*, Chapman & Hall, London 1993
[14] J. Klein, in *"Liquids at Interfaces"*, J. Charvolin, J.-F. Joanny, J. Zinn-Justin, Eds., North-Holland, Amsterdam 1990
[15] J. Klein, E. Kumacheva, D. Perahia, D. Mahalu, S. Warburg, *Faraday Discuss.* **98**, 174 (1994)
[16] J. Baschnagel, K. Binder, preprint
[17] A. Milchev, K. Binder, preprint
[18] R. Dickman, C. Hall, *J. Chem. Phys.* **89**, 3168 (1988)
[19] S. K. Kumar, M. Vacatello, D. Y. Yoon, *J. Chem. Phys.* **89**, 5206 (1988); *Macromolecules* **23**, 2189 (1990); M. Vacatello, F. Auriemma, *Macromol. Theory Simul.* **2**, 77 (1993); M. Vacatello, *Macromol. Theory Simul.* **3**, 325 (1994)
[20] D. N. Theodorou, *Macromolecules* **21**, 1391, 1400 (1988)
[21] A. Hertanto, R. Dickman, *J. Chem. Phys.* **93**, 774 (1990)
[22] A. Yethiraj, C. Hall, *Macromolecules* **23**, 1865 (1990)
[23] I. A. Bitsanis, G. Hadziioannou, *J. Chem. Phys.* **92**, 3827 (1990)
[24] R. Dickman, *Comput. Polym. Sci.* **1**, 206 (1991); *J. Chem. Phys.* **96**, 1516 (1992)
[25] A. Yethiraj, *J. Chem. Phys.* **101**, 2489 (1994); S. Phan, E. Kerlik, M. L. Rosinberg, A. Yethiraj, R. Dickman, *J. Chem. Phys.* **102**, 2141 (1995)
[26] G. B. McKenna, in *"Comprehensive Polymer Science"*, Vol. II, C. Booth, C. Price, Eds., Pergamon Press, New York 1988
[27] J. Zarzycki, Ed., *"Materials Science and Technology"*, Vol. IX, VCH Publ., Weinheim 1991
[28] J. Jäckle, *Rep. Prog. Phys.* **49**, 171 (1986)
[29] M. Wolfgardt, J. Baschnagel, K. Binder, *J. Chem. Phys.* **103**, 7166 (1995); M. Wolfgardt, J. Baschnagel, W. Paul, K. Binder, preprint
[30] I. Carmesin, K. Kremer, *Macromolecules* **21**, 2819 (1988); *J. Phys. (Paris)* **51**, 915 (1990)
[31] H.-P. Wittmann, K. Kremer, *Comput. Phys. Commun.* **61**, 309 (1990); *ibid.* **71**, 343 (1992)
[32] H.-P. Deutsch, K. Binder, *J. Chem. Phys.* **94**, 2294 (1991)
[33] W. Paul, K. Binder, D. W. Heermann, K. Kremer, *J. Phys. (Paris) II* **1**, 37 (1991)
[34] W. Paul, K. Binder, D. W. Heermann, K. Kremer, *J. Chem. Phys.* **95**, 7726 (1991)
[35] K. Binder, in *"Monte Carlo and Molecular Dynamics Simulations in Polymer Science"*, K. Binder, Ed., Oxford University Press, Oxford and New York 1995, Chap. 1
[36] H.-P. Deutsch, K. Binder, *Macromolecules* **25**, 6214 (1992); *Europhys. Lett.* **17**, 697 (1992)
[37] H.-P. Deutsch, K. Binder, *J. Phys. (Paris) II* **3**, 1049 (1993); H.-P. Deutsch, *J. Stat. Phys.* **67**, 1039 (1992)
[38] H.-P. Deutsch, K. Binder, *Makromol. Chem., Macromol. Symp.* **65**, 59 (1993); H.-P. Deutsch, *J. Chem. Phys.* **99**, 4825 (1993)
[39] M. Müller, K. Binder, *Comput. Phys. Commun.* **84**, 173 (1994); *Macromolecules* **28**, 1825 (1995)

[40] K. Binder, in *"Monte Carlo and Molecular Dynamics Simulations in Polymer Science"*, K. Binder, Ed., Oxford University Press, Oxford and New York 1995, Chap. 7
[41] P.-Y. Lai, K. Binder, *J. Chem. Phys.* **95**, 9288 (1991); *ibid.* **97**, 586 (1992)
[42] P.-Y. Lai, *J. Chem. Phys.* **98**, 669 (1993)
[43] P.-Y. Lai, K. Binder, *J. Chem. Phys.* **98**, 3366 (1993)
[44] J. Wittmer, A. Johner, J. F. Joanny, K. Binder, *J. Chem. Phys.* **101**, 4379 (1994)
[45] K. Binder, P.-Y. Lai, J. Wittmer, *Faraday Discuss.* **98**, 97 (1994)
[46] A. Kopf, J. Baschnagel, J. Wittmer, K. Binder, *Macromolecules*, in press
[47] H.-P. Wittmann, K. Kremer, K. Binder, *J. Chem. Phys.* **96**, 6291 (1992)
[48] J. Baschnagel, K. Binder, H.-P. Wittmann, *J. Phys.: Condens. Matter* **5**, 1597 (1993)
[49] J. Baschnagel, K. Binder, *Physica A* **204**, 47 (1994)
[50] B. Lobe, J. Baschnagel, K. Binder, *Macromolecules* **27**, 3654 (1994)
[51] M. Wolfgardt, J. Baschnagel, K. Binder, *J. Phys. (Paris) II* **5**, 1035 (1995)
[52] K. Binder, *Progr. Colloid Polym. Sci.* **96**, 7 (1994)
[53] W. Paul, J. Baschnagel, in *"Monte Carlo and Molecular Dynamics Simulations in Polymer Science"*, K. Binder, Ed., Oxford University Press, Oxford and New York 1995, Chap. 6
[54] J. Baschnagel, K. Binder, W. Paul, M. Laso, U. W. Suter, I. Batoulis, W. Jilge, T. Bürger, *J. Chem. Phys.* **95**, 6014 (1991)
[55] J. Baschnagel, K. Qin, W. Paul, K. Binder, *Macromolecules* **25**, 3117 (1992)
[56] K. Binder, *Makromol. Chem., Macromol. Symp.* **50**, 1 (1991)
[57] K. Binder, *Macromol. Symp.* **90**, 65 (1995)
[58] W. Paul, K. Binder, K. Kremer, D. W. Heermann, *Macromolecules* **24**, 6531 (1991); W. Paul, N. Pistoor, *Macromolecules* **27**, 1249 (1994)
[59] W. Paul, K. Binder, J. Batoulis, B. Pittel, K.-H. Sommer, *Makromol. Chem., Macromol. Symp.* **65**, 1 (1993)
[60] K. Binder, *Adv. Mater.* **4**, 540 (1992)
[61] P. E. Rouse, *J. Chem. Phys.* **21**, 127 (1953)
[62] M. Doi, S. F. Edwards, *"Theory of Polymer Dynamics"*, Clarendon Press, Oxford 1986
[63] P. J. Flory, *"Statistical Mechanics of Chain Molecules"*, Wiley, New York 1969
[64] J. Baschnagel, *Phys. Rev. B* **49**, 135 (1994); J. Baschnagel, M. Fuchs, *J. Phys. Condens. Matter* **7**, 6761 (1995)
[65] J. Baschnagel, in *"Transport Theory and Statistical Physics"*, Vol. 24, S. Yip, P. Nelson, Eds., Marcel Dekker, New York 1995, pp. 1249
[66] W. Petry, J. Wuttke, in *"Transport Theory and Statistical Physics"*, Vol. 24, S. Yip, P. Nelson, Eds., Marcel Dekker, New York 1995, pp. 1075; D. Richter, R. Zorn, B. Farago, B. Frick, L. J. Fetters, *Phys. Rev. Lett.* **68**, 71 (1992); B. Frick, B. Farago, D. Richter, *Phys. Rev. Lett.* **64**, 2921 (1990); D. Richter, B. Frick, B. Farago, *Phys. Rev. Lett.* **61**, 2465 (1988)
[67] W. Götze, L. Sjögren, in *"Transport Theory and Statistical Physics"*, Vol. 24, S. Yip, P. Nelson, Eds., Marcel Dekker, New York 1995, pp. 801; W. Götze, L. Sjögren, *Rep. Prog. Phys.* **55**, 241 (1992)
[68] H. Vogel, *Phys. Z.* **22**, 642 (1921); G. S. Fulcher, *J. Am. Ceram. Soc.* **8**, 339 (1925)
[69] F. Stickel, E. W. Fischer, R. Richert, *J. Chem. Phys.* **102**, 1 (1995); *J. Chem. Phys.*, in press
[70] P. G. De Gennes, *"Scaling Concepts in Polymer Physics"*, Cornell University Press, Ithaca 1979
[71] W. Rössler, H. Sillescu, in ref.[27], p. 573; H. Bässler, *Phys. Rev. Lett.* **58**, 767 (1987)
[72] K. Binder, A. Milchev, J. Baschnagel, *Annu. Rev. Mater. Sci.*, in press
[73] G. ten Brinke, D. Ausserre, G. Hadziioannou, *J. Chem. Phys.* **89**, 4374 (1988)
[74] K. F. Mansfield, D. N. Theodorou, *Macromolecules* **22**, 3143 (1989)
[75] W. G. Madden, *J. Chem. Phys.* **87**, 1405 (1987); *ibid.* **889**, 3934 (1988)

[76] J.-S. Wang, K. Binder, *J. Phys. (France) I* **1**, 1583 (1991)
[77] I. Bitsanis, G. ten Brinke, *J. Chem. Phys.* **99**, 3100 (1993)
[78] E. Donth, *J. Non-Cryst. Solids* **53**, 325 (1982)
[79] R. M. Ernst, S. R. Nagel, G. S. Grest, *Phys. Rev. B* **43**, 8070 (1991); C. Dasgupta, A. V. Indrani, S. Ramaswany, M. K. Phani, *Europhys. Lett.* **15**, 307 (1991)
[80] P. Ray, K. Binder, *Europhys. Lett.* **27**, 53 (1994)
[81] B. L. Holian, in *"Monte Carlo and Molecular Dynamics Simulations"*, K. Binder, G. Cicotti, Eds., Societa di Fisica Italiana, Bologna, in press
[82] S. Hess, in *"Monte Carlo and Molecular Dynamics Simulations"*, K. Binder, G. Cicotti, Eds., Societa di Fisica Italiana, Bologna, in press; P. A. Thompson, M. O. Robbins, G. S. Grest, *Phys. Rev. Lett.* **68**, 3448 (1992)
[83] D. Richter, K. Binder, B. Ewen, B. Stühn, *J. Chem. Phys.* **88**, 6618 (1984)
[84] I. A. Bitsanis, C. Pan, *J. Chem. Phys.* **99**, 5520 (1993); S. Gupta, D. C. Koopman, G. B. Westermann-Clark, I. A. Bitsanis, *J. Chem. Phys.* **100**, 8444 (1994)